15

The LDACS1 Physical Layer Design

Snjezana Gligorevic, Ulrich Epple and Michael Schnell
German Aerospace Center (DLR)
Oberpfaffenhofen,
Germany

1. Introduction

The legacy DSB-AM (Double Sideband Amplitude Modulation) system used for today's voice communication in the VHF-band is far away of meeting the demands of increasing air traffic and associated communication load. The introduction of VDL (VHF Digital Link) Mode 2 in Europe has already unfolded the paradigm shift from voice to data communication. Legacy systems, such as DSB-AM and VDL Mode 2 are expected to continue to be used in the future. However, they have to be supplemented in the near future by a new data link technology mainly for two reasons. First, only additional communication capacity can solve the frequency congestion and accommodate the traffic growth expected within the next 10-20 years in all parts of European airspace (ICAO-WGC, 2006). Second, the modernization of the Air Traffic Management (ATM) system as performed according to the SESAR (http://www.sesarju.eu/) and NextGen (http://www.faa.gov/nextgen/) programs in Europe and the US, respectively, heavily relies on powerful data link communications which VDL Mode 2 is unable to support.

Based on the conclusions of the future communications study (Budinger, 2011), the ICAO Working Group of the Whole (ICAO-WGW, 2008) has foreseen a new technology operating in the L-band as the main terrestrial component of the Future Communication Infrastructure (FCI) (Fistas, 2011) for all phases of flight. Hence, such L-band technology shall meet the future ATM needs in the en-route and the Terminal Manoeuvring Area (TMA) flight domains as well as within airports. The latter application area will be supplemented by the AeroMACS technology at many large airports (Budinger, 2011).

A final choice of technology for the L-band has not been made yet. Within the future communications study, various candidate technologies were considered and evaluated. However, it was found that none of the considered technologies could be fully recommended before the spectrum compatibility between the proposed systems and the legacy systems has been proven. This will require the development of prototypes for testing in a real environment against operational legacy equipment.

The future communications study has identified two technology options for the L-band Digital Aeronautical Communication System (LDACS) as the most promising candidates for meeting the requirements on a future aeronautical data link. The first option, named LDACS1, is a Frequency-Division Duplex (FDD) configuration utilizing Orthogonal Frequency-Division Multiplexing (OFDM), a highly efficient multi-carrier modulation technique which enables the use of higher-order modulation schemes and Adaptive Coding and Modulation (ACM). OFDM has been adopted for current and future mobile radio communications technologies, like 3GPP LTE (Third Generation Partnership Project Long Term Evolution) and 4G (Fourth Generation mobile radio system). In addition, LDACS1 utilizes reservation based access control (Gräupel & Ehammer, 2011) to guarantee timely channel access for the aircraft and advanced network protocols similar to WiMAX (Worldwide Interoperability for Microwave Access) and 3GPP LTE to ensure high quality-of-service management and efficient use of communication resources. LDACS1 is closely related to the Broadband Aeronautical Multi-Carrier Communication (B-AMC) and TIA-902 (P34) technologies (Haindl at al., 2009).

LDACS2 is the second option which is based on a single-carrier technology. It utilizes a binary modulation derivative (Continuous-Phase Frequency-Shift Keying, CPFSK) and thus does not enable the use of higher-order modulation schemes. For duplexing Time-Division Duplex (TDD) is chosen. The physical layer has some similarities to both the Universal Access Transceiver (UAT) and the second generation mobile radio system GSM (Global System for Mobile Communications). A custom protocol is used providing high quality-of-service management capability. This option is a derivative of the L-band Data Link (LDL) and the All-purpose Multi-channel Aviation Communication System (AMACS) technologies (EUROCONTROL, 2007).

Follow-on activities required in order to validate the performance of the proposed LDACS options and their compatibility with legacy L-band systems, finally aiming at a decision on a single L-band technology, run under the SESAR framework (http://www.sesarju.eu/; Fistas, 2011).

2. System requirements

The choice of the radio link is based on the capacity the link should provide related primarily to the services and applications that it should support. The radio frequency will affect the propagation loss, whereas the channel fading in a deterministic environment may also vary with the system bandwidth. Additionally, the interference conditions in the part of the L-band assigned to the Aeronautical Mobile (Route) Service (AM(R)S) have to be considered. Consequently, the development of an air-ground data link in the L-band faces several requirements, both operational and technical.

2.1 Services and applications

Air Traffic Services (ATS) and Airline Operational Communications (AOC) services are related to safety and regularity of flight and hence entail more stringent requirements on a future communication system in comparison with commercial mobile communication systems.

One of the requirements for a new data link in the L-band is the suitability to support future services and applications as described in (EUROCONTROL & FAA, 2007). The document describes safety, information security, and performance assessments for the air traffic services, derives high-level requirements that each service would have to meet and allocates the requirements to the future radio system. Beside a range of parameters on which the suitability of communication systems can be assessed, the document provides capacity requirements estimated for different service volumes and regarding increasing air traffic and future communication concepts.

2.2 Propagation conditions

Typically, during the flight an aircraft traverses numerous Air Traffic Control (ATC) sectors and en-route facilities. In comparison to the VHF band used by the legacy ATC systems, higher free space loss in the L-band implies smaller sector sizes. The possibility of increasing transmitter (Tx) power is limited by the interference constraints and the amplifier dimensions. Hence, the reuse factor of the cellular LDACS system and the interference constraints within the L-band should be taken into account not only for the link budget calculation but also for frequency planning for the European airspace.

Furthermore, the sector size affects the system capacity in terms of data throughput per aircraft, but also the system design in terms of required guard times between Forward Link (FL) and Reverse Link (RL). Whereas in the FDD configuration, as for LDACS1, the guard times have to be guaranteed only in the random access phase, the general requirement for guard times in a TDD based system implies a loss in the system capacity.

In en-route domain, propagation conditions are characterized by a very strong Line-Of-Sight (LOS) component, and thus, multipath effects have only very limited influence on the received signal quality. More severe multipath conditions in the TMA and airport domains result in increased frequency selectivity of the channel. A broadband system may benefit from the frequency diversity related to the multipath, whereas a narrowband system will be affected by more severe fading on the LOS path between transmitter and receiver.

According to the publications on propagation conditions in L-band based on measurements (Rice et al, 2004) and on theoretical considerations (ICAO-WGC, 2006), the Root Mean Square Delay Spread (RMS-DS) remains below 2 μs in en-route case. The maximum delay and delay spread increase in TMA and airport areas. Measurements at airports provide a maximum RMS-DS of 4.5 μs and 90^{th} percentile delay spread not exceeding 1.7 μs during taxiing (Gligorevic et al., 2009; Matolak et al., 2008).

Taking into account an aircraft velocity of 1050 km/h in an en-route area we obtain a maximum Doppler frequency of 972 Hz. However, due to the dominant LOS component in en-route domain, the Doppler effect will mainly cause a Doppler shift of the carrier frequency. Since the velocity is lower in TMA and especially in airport areas, the Doppler spread resulting from the Doppler effect in the reflections of the signal will be lower. According to (Bello, 1973), the reflections in the L-band can be modelled as a Rayleigh process with a Gaussian Doppler spectrum.

2.3 Spectrum

LDACS shall operate in the lower part of the L-band, 960 - 1164 MHz. As depicted in Fig. 1, the L-band is already utilized by several systems.

The Distance Measuring Equipment (DME) operating as an FDD system on the 1 MHz channel grid is a major user[1] of the L-band. Parts of this band are used in some countries by the military Multifunctional Information Distribution System (MIDS). Several fixed channels are allocated for the Universal Access Transceiver (UAT) and the Secondary Surveillance Radar (SSR)/Airborne Collision Avoidance System (ACAS). Fixed allocations have been made in the upper part of the L-band for the Global Position System (GPS), Global Orbiting Navigation Satellite System (GLONASS) and GALILEO channels. The commercial mobile radio systems UMTS (Universal Mobile Telecommunications System) and GSM are operating immediately below the lower boundary of the aeronautical L-band (960 MHz). Additionally, different types of RSBN (Радиотехническая система ближней навигации is a Russian air navigation system)

[1]DME channels are also used by the military Tactical Air Navigation (TACAN) system.

may be found in some parts of the world, operating on channels 960 - 1164 MHz (SESAR JU, 2011).

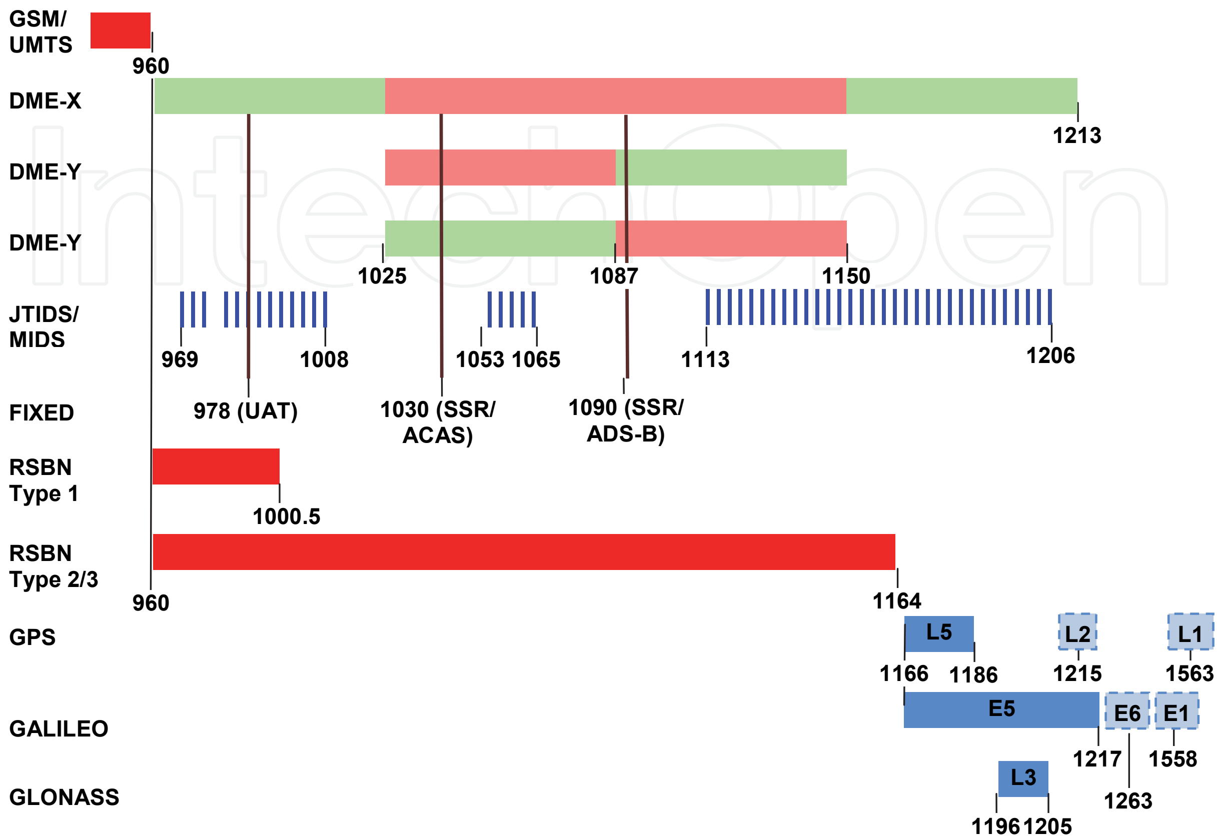

Fig. 1. Current L-band usage (SESAR JU, 2011).

The DME-free part of the spectrum is only between 960 – 975 MHz. Both LDACS systems can use this spectrum of 15 MHz proving not to interfere with the adjacent GSM and UMTS in the lower band, UAT at 978 MHz, and ground DME above 978 MHz. Whereas LDACS2 is expected to operate in the 960-975 MHz frequency band, LDACS1 offers also the opportunity to use spectral gaps between existing DME channels, thus increasing the potential number of communication channels. In this inlay deployment option LDACS1 operates at only 500 kHz offset to assigned DME channels as exemplarily shown in Fig. 2.

One of the challenges to build up a cellular system is to find a sufficient number of channels. In case of LDACS1, RL (air to ground) and FL (ground to air) are separated by FDD. When selecting channels for LDACS1, co-location constraints have to be considered for the aircraft equipment. Additionally, the fixed L-band channels at 978, 1030, and 1090 MHz must be sufficiently isolated from LDACS1 channels by appropriate guard bands. To relax co-site interference problems for an airborne LDACS1 receiver (Rx) in the inlay deployment option, the frequency range 1048.5 - 1171.5 MHz, which is currently used by airborne DME interrogators, should be used for the RL, i.e. airborne LDACS1 Tx. The proposed sub-range for the FL is 985.5 - 1008.5 MHz, i.e. at 63 MHz offset to the RL which corresponds to the DME duplex spacing.

The inlay concept offers the clear advantage that it does not require new channel assignments and the existing assignments can remain unchanged. The physical layer design of LDACS1, described in the following section, accounts primarily for the inlay concept aiming for coexistence with DME system operating on adjacent channels. However, the LDACS1 design also allows a non-inlay or a mixed inlay/non-inlay deployment without any modifications.

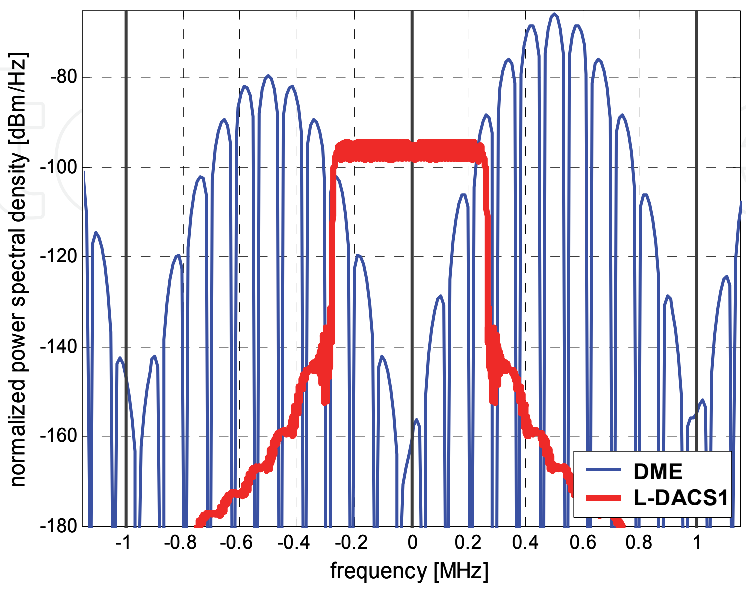

Fig. 2. An example of LDACS1 spectrum and DME interference in the inlay deployment scenario.

3. LDACS1 physical layer characteristics

The LDACS1 physical layer is based on OFDM modulation and designed for operation in the aeronautical L-band (960 – 1164 MHz). Aiming for the challenging inlay deployment option, with limited bandwidth of around 500 kHz available between successive DME channels, and in order to maximize the capacity per channel and optimally use available spectrum, LDACS1 is configured as a FDD system. A TDD approach would be less efficient, since it would require large guard times due to the propagation delays and a split of the available bandwidth into FL and RL transmission. Furthermore, by properly choosing FL and RL frequencies from appropriate parts of the L-band, the co-location interference situation on the aircraft can be significantly relieved.

LDACS1 FL is a continuous OFDM transmission. Broadcast and addressed user data are transmitted on a (logical) data channel, dedicated control and signaling information is transmitted on (logical) control channels. The capacity of the data and the control channel changes according to system loading and service requirements. Message based adaptive data transmission with adjustable modulation and coding parameters is supported for the data channels in FL and RL.

LDACS1 RL transmission is based on Orthogonal Frequency-Division Multiple Access (OFDMA) – Time-Division Multiple Access (TDMA) bursts assigned to different users on demand. In particular, the RL data and the control segments are divided into tiles, hence allowing the Medium-Access Control (MAC) sub-layer of the data link layer to optimize the resource assignments as well as to control the bandwidth and the duty cycle according to the interference conditions.

The channel bandwidth of 498.05 kHz is used by an OFDM system with 50 subcarriers. The resulting subcarrier spacing of 9.765625 kHz is sufficient to compensate a Doppler spread of up to about 1.25 kHz which is larger than typically occurring at aeronautical velocities. For OFDM modulation, a 64-point FFT is used. The total FFT bandwidth comprising all subcarriers is 625.0 kHz.
According to the subcarrier spacing, one OFDM symbol has duration of 102.4 µs. Each OFDM symbol is extended by a cyclic prefix of 17.6 µs, comprising a guard interval of 4.8 µs for compensating multipath effects and 12.8 µs for Tx windowing applied for reduction of the out-of-band radiation. This results in a total OFDM symbol duration of 120 µs. The main LDACS1 OFDM parameters are listed in Table 1.

Parameter	Value
Effective bandwidth (FL or RL)	498.05 kHz
Subcarrier spacing	9.765625 kHz
Used subcarriers	50
FFT length	64
OFDM symbol duration	102.4 µs
Cyclic prefix Guard time Windowing time	17.6 µs 4.8 µs 12.8 µs
Total OFDM symbol duration	120 µs

Table 1. Main LDACS1 OFDM parameters.

3.1 Frame structure

The 64 subcarriers in the FFT bandwidth are assigned to different types of symbols providing different functionalities:

- Null symbols are not transmitted. In most frame types, seven subcarriers on the left and six on the right hand side of the spectrum carry null symbols and serve as guard bands. In addition, the subcarrier in the center (DC subcarrier) of the spectrum is not transmitted.
- Pilot symbols are known in advance, exploited in the receiver for estimating the transmission channel.
- Symbols for reducing the Peak-to-Average Power Ratio (PAPR) are determined depending on the data in the respective OFDM symbol. PAPR reduction symbols are used in RL only.
- Synchronization symbols are used to obtain time and frequency synchronization in the receiver.
- Preamble symbols are used for facilitating receiver Automatic Gain Control (AGC).
- Data symbols are used for data transmission.

Multiple OFDM symbols are organized into frames. Depending on their functionality and on the link direction, different frame types are distinguished.

3.1.1 FL OFDM frame types

In the FL, BroadCast (BC) and combined Data/Common Control (CC) frames are utilized. The FL Data/CC frame comprises 50 subcarriers with 54 OFDM symbols, starting with two

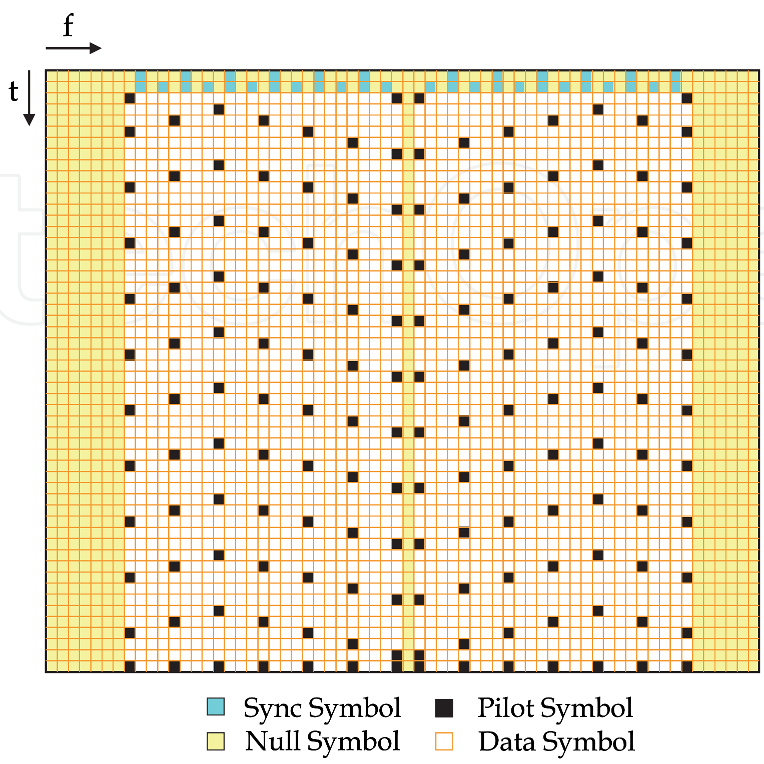

Fig. 3. Structure of a FL Data/CC frame.

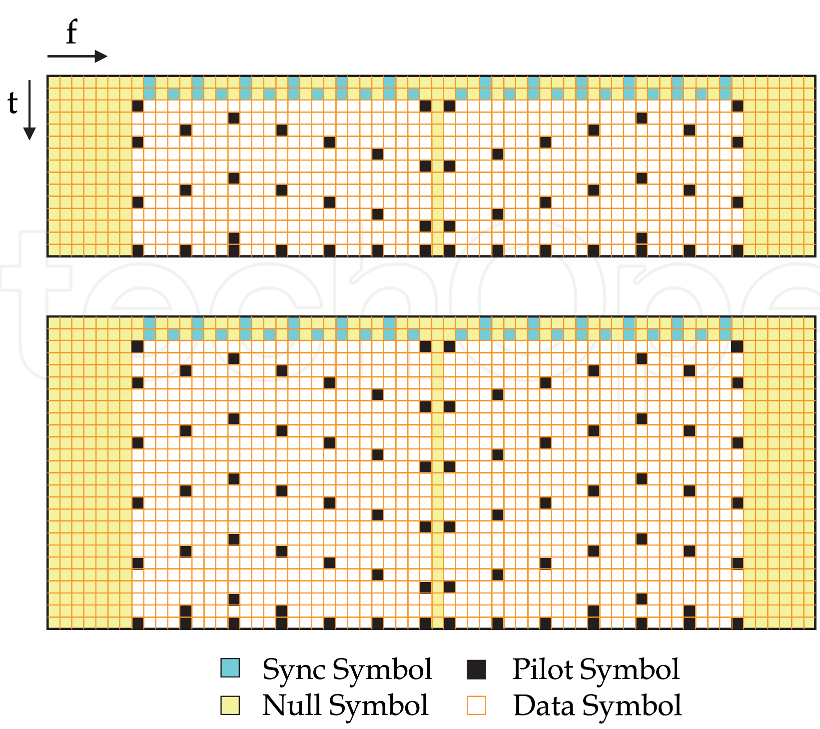

Fig. 4. Structure of BC1 and BC3 sub-frames (above) and BC2 sub-frame (below).

synchronization OFDM symbols followed by 52 OFDM symbols carrying data and pilot symbols, as depicted in Fig. 3. Subtracting the total number of 158 pilot symbols results in a total data capacity of 2442 symbols per FL Data/CC frame. The mapping of CC information and data onto this frame type is described later in this section.
An FL BC frame consists of three consecutive sub-frames (BC1/BC2/BC3), in which the Ground Station (GS) broadcasts signaling information to all active Airborne Stations (ASs) within its coverage range. Fig. 4 shows the structure of these sub-frames. In the BC1 and BC3 sub-frames, two of 15 OFDM symbols are used for synchronization. In the remaining 13 OFDM symbols, 48 carriers are modulated by pilot symbols and 602 remain for data transmission. The BC2 sub-frame is eleven OFDM symbols longer than the BC1/3 sub-frame and provides a capacity of 1120 data symbols.
Note that in the FL frames, no PAPR reduction symbols are inserted as the power amplifier used in the GS is assumed to provide sufficient linearity.

3.1.2 RL OFDM frame types

To realize multiple-access via OFDMA-TDMA in the RL, the transmission is organized in segments and tiles rather than in OFDM frames and sub-frames as in the FL. The usage of tiles enables the optimization of the resource assignments by the MAC sub-layer. Furthermore, bandwidth and duty cycle can be optimally selected according to the interference conditions.
As illustrated in Fig. 5, one tile, representing the smallest allocation block in the RL, spans 25 symbols in frequency and six symbols in time direction in the time-frequency plane. It comprises four PAPR reduction symbols and twelve pilot symbols. This leads to a data capacity of 134 data symbols per tile.

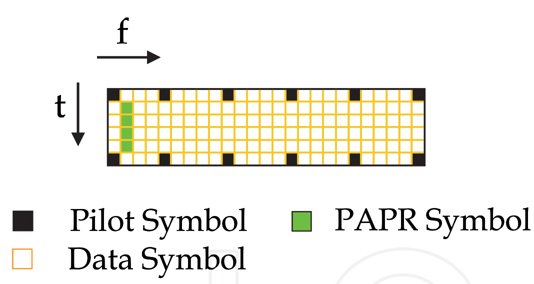

Fig. 5. Structure of a data tile in the RL.

The values of the PAPR reduction symbols are optimized in dependence on the data content such that the entire OFDM symbol, i.e. 24 data symbols and one PAPR reduction symbol, produces a minimal PAPR. In the first and the last OFDM symbol in a tile, PAPR is minimized by optimizing the phases of the pilot symbols in a way that the contribution of the pilot symbols to the PAPR is minimal.
The tiles of the data segment are subsequently positioned left of the DC subcarrier and mirrored versions of the tiles are positioned right of the DC subcarrier. The length of the data segment is kept variable by allocating a variable number of tiles to the data segment. This structure also supports a flexible assignment of resources to different ASs by assigning different tiles or different blocks of subsequent tiles to different ASs.
Signaling information like resource allocation requests is transmitted in the Dedicated Control (DC) segment. A DC segment has the same tile structure as the RL data segment.

However, it starts with a so called synchronization tile, spanning five OFDM symbols in time direction and 51 subcarriers, including the DC subcarrier, in frequency direction. The synchronization tile as illustrated in Fig. 6 starts with an AGC preamble, followed by two OFDM synchronization symbols. The forth and fifth OFDM symbol consist of pilot symbols only. This synchronization tile provides a possibility for an AS to execute seamless handover, when entering a new LDACS1 cell.

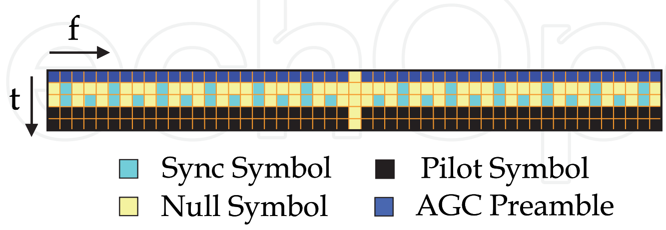

Fig. 6. Structure of one synchronization tile.

After the synchronization tile, an AGC preamble is inserted in the DC segment. This additional AGC preamble is necessary, since an AS, performing seamless handover is not yet power-controlled with the new GS, leading to a different power level at the receiving GS, compared to the signals from the other ASs. Within the remainder of the DC segment, exactly one tile is assigned to each AS within the cell. The preceding AGC preamble is transmitted by the same AS which transmits the first tile in the DC segment. The length of a DC segment is variable, depending on the number of ASs within the LDACS1 cell. As an example, one DC segment comprising six tiles corresponding to six active ASs within one cell, is depicted in Fig. 7.

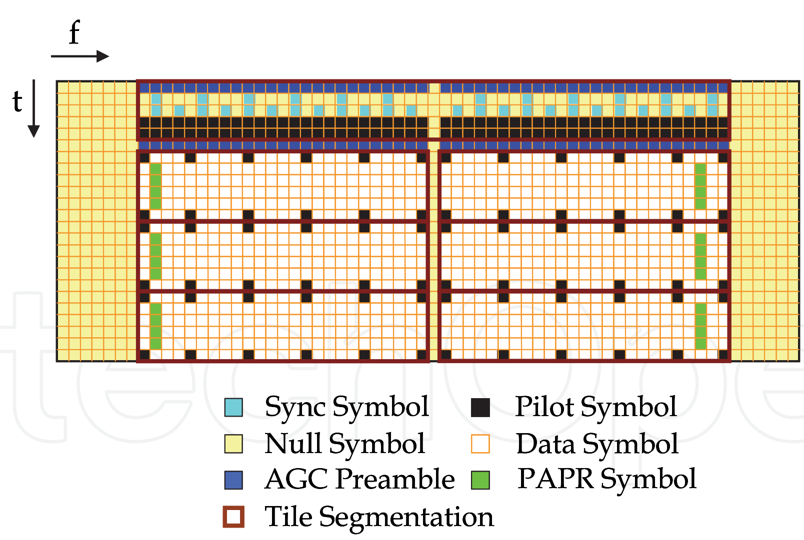

Fig. 7. Structure of one DC segment.

Besides the mentioned seamless handover, LDACS1 provides additional opportunities for handover by means of two consecutive RL Random Access (RA) opportunities, in which an AS can send its cell entry request to the GS (see Fig. 8). Propagation guard times of up to 1.26 ms precede and follow each RA frame. The propagation guard time of 1.26 ms corresponds to a maximal AS-GS distance of 200 nm. When transmitting a cell entry request, an AS is not yet synchronized to the GS, which means that the distance between the AS and the GS is unknown. Hence, the distance can take values up to 200 nm which corresponds to the maximum LDACS1 cell size. The unknown propagation time differences are well compensated by the inserted guard times, guaranteeing that the cell entry request does not superimpose at the receiving GS with signals from other ASs within the cell.

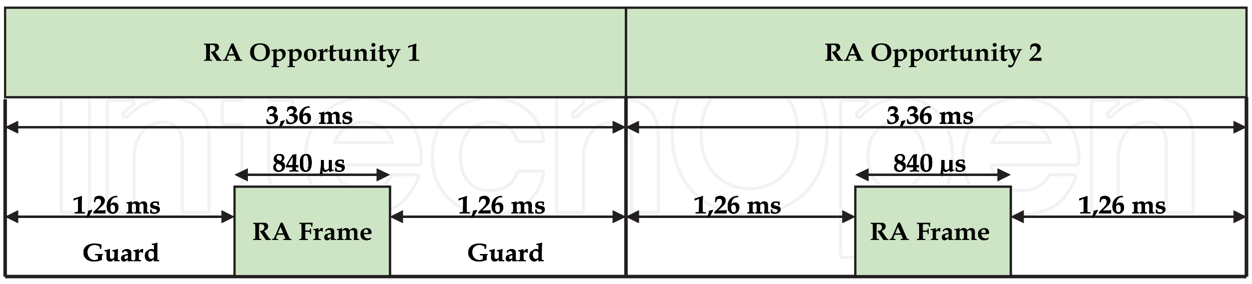

Fig. 8. Random access opportunities.

In Fig. 9, the structure of a RA frame itself is depicted. The first OFDM symbol represents the AGC preamble, the following two OFDM symbols contain synchronization sequences, while the remaining four OFDM symbols carry data, PAPR reduction symbols and pilot symbols. These four OFDM symbols use only 27 subcarriers (including the DC subcarrier), which leads to larger guard bands with 19 empty subcarriers on the left side and 18 on the right side.

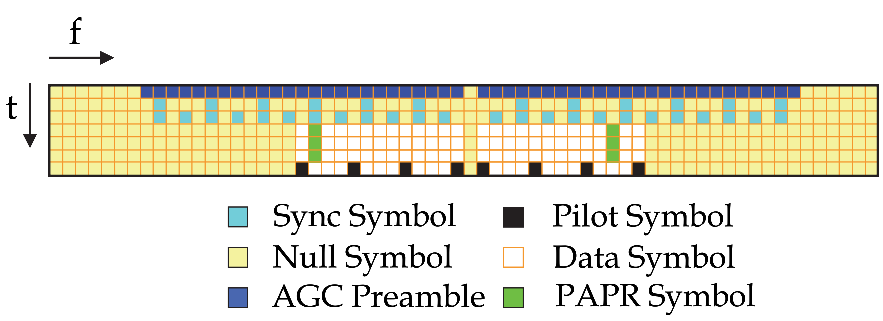

Fig. 9. Structure of random access frame.

3.1.3 Framing structure

In the FL, nine CC/Data frames are combined to one Multi-Frame (MF). The assignment of the nine frames within one MF either for user data or for common control information is variable. Starting with the fifth frame, one up to four frames can be allocated for common control information. The remaining frames contain user data. The mapping of modulated symbols onto the frames is performed block wise. These blocks are called Physical layer Protocol Data Units (PHY-PDUs). In general, three PHY-PDUs are mapped onto one Data/CC frame in FL MFs.
Each MF in the RL starts with a RL DC segment, followed by a RL data segment. The size of the DC segment, and thus also the size of the data segment is variable. The minimum size DC segment comprises one synchronization tile and the subsequent AGC preamble, followed by two tiles, corresponding to the case of one or two ASs within the cell. Since the extension of the DC segment over the entire MF is not reasonable, the maximum size of the DC segment is limited to 52 tiles. The remainder of the frame is filled up with the data segment. In the RL, one PHY-PDU is always mapped onto one tile.

The MF structure for FL and RL is shown in Fig. 10. The reference synchronization point for the FL and RL is the beginning of the MF. It is noticeable that the common control information in the FL and the dedicated control information in the RL are transmitted interleaved rather than simultaneously. The temporal shift of the FL control information allows the requests sent in the RL DC segment to be answered already in the FL CC frames of the same MF. Similarly, resource allocations transmitted in the FL CC frames can already be used in the next RL MF.

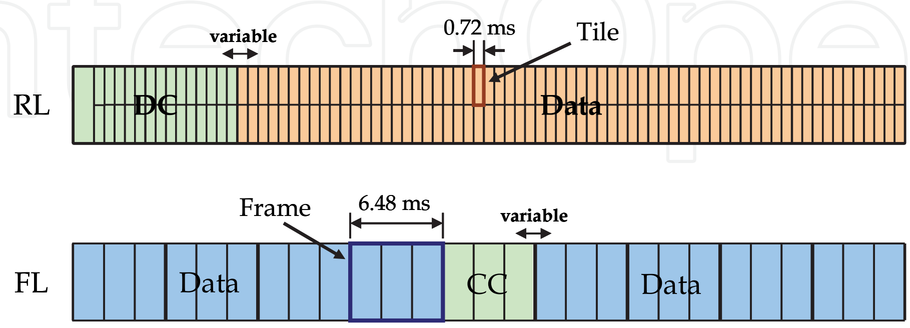

Fig. 10. Multi-Frame structures.

On top of the MF structure, a Super-Frame (SF) structure is provided. In the FL, one SF contains a BC frame of duration 6.72 ms, and four MFs, each of duration 58.32. In the RL, each SF starts with two opportunities for transmitting RL RA frames followed by four MFs. The start of the FL BC frame is synchronized to the start of the RL RA. The SF structure is summarized graphically in Fig. 11.

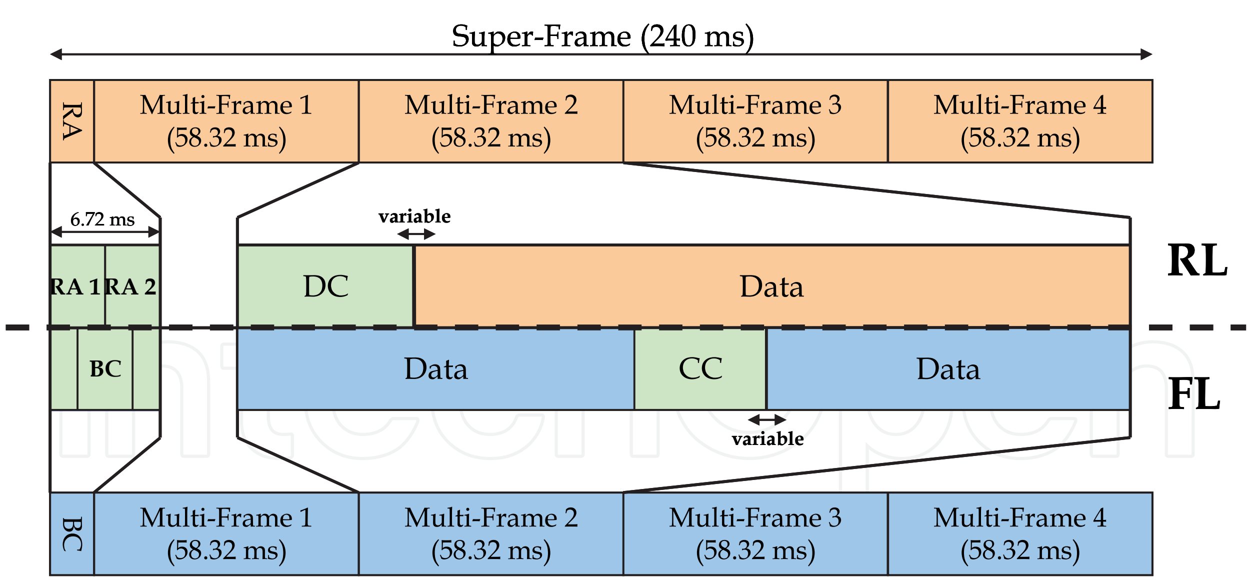

Fig. 11. Super-Frame Structure.

3.2 Coding and modulation

Different robust coding schemes proposed for LDACS1 should cope with the interference the transmit signal is exposed to. Primarily for small coding block sizes, a convolutional code of rate 1/3, followed by a bit interleaver is defined. For larger coding block sizes, a concatenated coding scheme consisting of a rate 0.9 Reed-Solomon (RS) code and a rate 1/2 convolutional code is employed. Again, the convolutional coder is followed by a bit interleaver. In addition, a byte interleaver between the two coders is inserted. The rate of the convolutional code can be changed from 1/2 to 2/3 or 3/4 by puncturing. The coding scheme is depicted in Fig. 12.

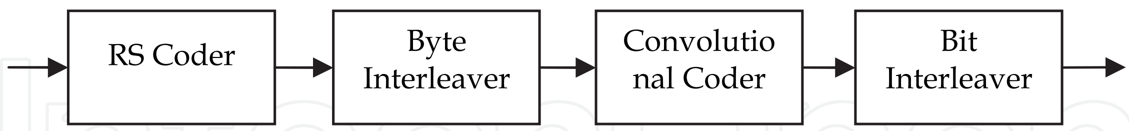

Fig. 12. Concatenated coding scheme.

For the subsequent modulation, Quaternary Phase-Shift Keying (QPSK) modulation, 16 Quadrature Amplitude Modulation (QAM), and 64 QAM are available.
The coding rates and the modulation scheme in the data frames can be adapted, based on the current channel and interference conditions, maximizing the transmission capacity. Therefore two Adaptive Coding and Modulation (ACM) modes are defined:

- Cell-specific ACM mode, which means that data for all users within one cell are encoded and modulated with a fixed scheme, and
- User-specific ACM mode, which means that separate coding and modulation schemes are applied for the data of different users.

In both modes, QPSK, 16QAM, and 64QAM are available. The rate of the convolutional code can be changed from 1/2 to 2/3 or 3/4. From the possible 9 combinations 8 are available[2] as ACM schemes.
For the particular frame types, the following coding and modulation scheme is chosen:

- In FL data frames, the concatenated coding scheme is mandatory. The coding rate and the modulation scheme is variable, both ACM modes are available. In case of cell-specific ACM, the information about the chosen coding and modulation scheme is transmitted in the BC frame. In case of user-specific ACM, the GS transmits the information about coding and modulation for different ASs via the coding and modulation scheme FL map in the CC information block.
- In RL data segments, the concatenated coding scheme is mandatory. The coding rate and the modulation scheme is variable, user-specific ACM is available. The selection of a coding and modulation scheme for a certain AS is carried out by the GS and communicated when assigning resources to this AS.
- For the BC sub-frames and the CC frames, again the concatenated coding scheme is employed. To guarantee an adequate protection of the control information, convolutional coding rate 1/2 and QPSK modulation is mandatory.
- The data in the RA frames and DC segment is encoded with the rate 1/3 convolutional coder, which is suitable for the small block sizes in these frames. QPSK modulation scheme is mandatory.

3.3 Reduction of out-of-band radiation

High out-of-band OFDM side lobes may cause harmful interference at the Rx of other L-band systems and have to be reduced. For that purpose, Tx windowing is applied in order to smooth the sharp phase transitions between consecutive OFDM symbols which cause out-of-band radiation.

[2]Only the combination of 16QAM with rate 3/4 coding has been omitted.

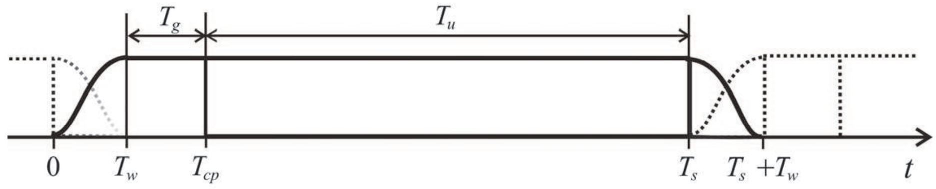

Fig. 13. Tx windowing principle.

As illustrated in Fig. 13, the OFDM symbol is extended by a cyclic prefix of total length T_{cp}=T_w+T_g. One part of the cyclic prefix serves as guard interval of length T_g to compensate multipath propagation on the radio channel. The second part is of length T_w and contains the leading edge of the window. In addition, the OFDM symbol is extended by a cyclic suffix which contains the trailing edge of the window of length T_w. This approach guarantees that Tx windowing does not affect the useful part of the OFDM symbol including guard interval. To keep the overhead induced by extending the OFDM symbol duration at a minimum, subsequent OFDM symbols overlap in those parts containing the leading and trailing edges of the window. For LDACS1, a raised-cosine window with roll-off factor α = 0.107 is proposed.

3.4 Receiver design

When deployed as an inlay system, signals of existing L-band systems may cause severe interference onto the LDACS1 Rx. Especially DME systems operating at a small frequency offset to the LDACS1 channel represent a source of strong interference. Two promising techniques, aiming at mitigation of the influence of interference onto LDACS1, are presented in the following. In addition, the effect of the interference and the proposed interference mitigation to the estimation of the transmission channel is examined.

3.4.1 Over-sampling

RF and IF filters in the selective stages of the LDACS1 Rx successively reduce interference contributions received outside the LDACS1 bandwidth. Since the interference signal power can be very high, it may be impossible to completely remove this out-of-band interference power. In particular, due to the relatively large occupied bandwidth of the DME signal, the spectra of DME Txs operating at ±0.5 MHz offset from the LDACS1 channel partly fall into the LDASC1 Rx bandwidth. Subsequent sampling of the filtered Rx signal in the A/D-converter with the native sampling period leads to periodic repetitions of the interference spectra in the frequency domain in distances of multiples of the FFT bandwidth B_{FFT}. In the case without interference, the filtered Rx signal is band-limited by B_{FFT}. Sampling with $T_{\mathrm{sa}} = 1/B_{FFT}$ does not lead to aliasing effects. However, the Nyquist sampling theorem is not fulfilled for the interference signal. The remaining out-of-band interference signal is not band-limited to B_{eff}, hence due to aliasing after Rx FFT operation the undesired signal parts fall into the LDACS1 bandwidth. This can be avoided by over-sampling the time domain Rx signal at least by a factor of four, resulting in an increased spacing between the periodic repetitions in the frequency domain and reduced aliasing effects. The over-sampled Rx signal is then transformed to the frequency domain by FFT with the size increased according to the over-sampling factor. For further signal processing, only the relevant subcarriers in the LDACS1 system bandwidth are considered. All other subcarriers are discarded.

3.4.2 Pulse blanking

Pulse Blanking (PB) is a well-known approach for reducing pulsed interference such as DME interference. It has already been applied for reducing DME interference in the E5- and L5-bands used by satellite navigation systems (Gao, 2007) and for reducing impulsive noise in OFDM systems (Zhidkov, 2006).

In LDACS1, PB is applied to the digitized Rx signal after A/D conversion. When the amplitude of the over-sampled Rx signal exceeds a pre-defined threshold T_{PB} the corresponding samples are blanked, i.e. set to zero. Besides the DME interference, the blanked samples also comprise the desired OFDM signal and noise. Hence, the threshold T_{PB} has to be chosen carefully. When choosing it too low, the corruption of the desired signal exceeds the benefit of reducing the interference power, whereas a too high threshold leads to a strong remaining interference power. A suitable criterion for optimally setting T_{PB} is the Signal-to- Interference-and-Noise ratio (SINR) (Zhidkov, 2006).

Due to high PAPR in OFDM systems, peaks of the desired OFDM signal and DME pulses cannot be clearly distinguished. For an unambiguous detection of interference pulses in the Rx signal, a correlation of the Rx signal with a known interference pulse has been proposed in (Brandes & Schnell, 2009).

An algorithm for diminishing the harmful PB influence onto the useful OFDM signal was presented in (Brandes et al., 2009). It is based on the idea, that the PB impact on the OFDM signal can be determined exactly when representing PB as a windowing operation. The window function is a rectangular window that exhibits notches at those positions where the Rx signal is blanked. Recalling that the shape of the window determines the spectrum of the OFDM subcarriers, the subcarrier spectra can be determined and the distortion induced by PB is identified as Inter-Carrier Interference (ICI). ICI can easily be reduced by subtracting the known impact of all other subcarriers from the considered subcarrier as applied for example for reducing ICI in OFDMA systems induced by frequency offsets (Fantacci et al., 2004).

3.4.3 Channel estimation

As basic channel estimation algorithm in LDACS1, a pilot-aided linear interpolation is proposed. In order to make channel estimation robust towards interference the pilot tones in frequency direction are spread over all subcarriers in order to reduce the number of pilot tones that would be affected by a strong DME interference pulse from the adjacent DME channel. In RL, such pilot tone placing is not possible due to the OFDMA approach. In this case the pilot tones have to be placed of the edges of each tile. These pilot distances in time and frequency direction have been chosen in accordance with the expected Doppler shifts and maximal delay times in the case of multipath propagation. To improve channel estimation, pilot boosting is applied. In this case, the power of the pilot symbols is increased by 4 dB over the average power of each data symbol.

A more sophisticated approach for estimating the transmission channel is Wiener filtering. The coefficients of the Wiener interpolation filter are derived by minimizing the Mean-Squared-Error (MSE) between the actual and the estimated channel coefficients. This leads to an optimal noise suppression, given the noise variance and channel statistics. In (Epple & Schnell, 2010), it was proposed to incorporate an equivalent noise term, comprising the additive white Gaussian noise and the estimated DME interference, into the Wiener filter. If interference mitigation like PB is applied, the variance of the induced ICI can be incorporated into the Wiener filtering (Epple et al., 2011). Both approaches turned out to improve the channel estimation performance remarkably.

4. Conclusion

LDACS1 is the broadband candidate for the future L-band communications system which covers the air-ground link within the FCI. The design of LDACS1 is based on the multi-carrier technology OFDM, a modern communications technology which is highly flexible and efficient. In comparable application domains, like mobile radio communications, OFDM is the current state-of-the-art solution and is also foreseen for the next generation of mobile radio systems.

The LDACS1 design is based on existing multi-carrier standards, like WiMAX and P34. However, due to the operational requirements on an aeronautical communications system, the propagation conditions, and the interference environment in L-band a specific OFDM solution had to be designed. Investigations of the LDACS1 system performed by computer simulations have proven the suitability of the LDACS1 design for use in the L-band (Brandes et al., 2009; Epple & Schnell, 2010; Epple et al., 2011). Even for the challenging inlay deployment scenario, LDACS1 is expected to work according to the requirements without causing harmful interference to the legacy L-band systems. With that, LDACS1 shows that aeronautical communications can profit from the developments in related fields and can achieve efficient usage of the scarce spectrum resources currently available for communications within aviation.

5. References

Bello P.A. (1973). Aeronautical Channel Characterization, *IEEE Trans. on Communications*, vol. COM-21, no 5, pp. 548-563, May 1973

Brandes, S.; Epple, U. & Schnell, M. (2009). Compensation of the Impact of Interference Mitigation by Pulse Blanking in OFDM Systems, *Proceedings of IEEE Global Telecommunications Conference 2009*, Honolulu, Hawaii, USA, November 28-December 4, 2009

Brandes, S. & Schnell, M. (2009). Interference Mitigation for the Future Aeronautical L-Band Communication System, *Proceedings of 7th International Workshop on Multi-Carrier Systems & Solutions 2009*, Herrsching, Germany, May 5-6, 2009

Budinger J.M. (2011). Aeronautical Mobile Airport Communications System (AeroMACS), Future Aeronautical Communications, Simon Plass (ed.), ISBN 979-953-307-443-5

Epple, U.; Shibli, K. & Schnell, M. (2011). Investigation of Blanking Nonlinearity in OFDM Systems, *Proceedings of IEEE International Communications Conference 2011*, Kyoto, Japan, June 5-9, 2011

Epple, U. & Schnell, M. (2010). Channel Estimation in OFDM Systems with Strong Interference, *Proceedings of 15th International OFDM Workshop 2010*, pp. 26-30, Hamburg, Germany, September 1-2, 2010

EUROCONTROL (2007). Future Communications Infrastructure - Technology Investigations. Description of AMACS, v1.0, 2007. Available from http://www.eurocontrol.int/communications/public/standard_page/LBANDLIB.html. Information available also on http://www.eurocontrol.int

EUROCONTROL & FAA (2007). Communications Operating Concept and Requirements for the Future Radio System, (COCR) version 2

Fantacci, R.; Marabissi, D. & Papini, S. (2004). Multiuser Interference Cancellation Receivers for OFDMA Uplink Communications with Carrier Frequency Offset, *Proceedings of IEEE Global Telecommunications Conference 2004*, pp. 7081-7085, Dallas, Texas, USA, November 29-December 3, 2004

Fistas N. (2011). Aeronautical Future Aeronautical Communications: The Data Link Component, Future Aeronautical Communications, Simon Plass (ed.), ISBN 979-953-307-443-5

Gao, G.X. (2007). DME/TACAN Interference and its Mitigation in L5/E5 Bands, *Proceedings of ION Institute of Navigation Global Navigation Satellite Systems Conference*, Fort Worth, Texas, USA, September 25-28, 2007

Gligorevic, S., Zierhut, R., Jost, T., Wang, W. (2009). Airport Channel Measurements at 5.2GHz, *In Proceedings of the 3rd European Conference on Antennas and Propagation (Eucap),* March 2009

Gräupel T. & Ehammer M. (2011). The LDACS1 Link Layer Design, Future Aeronautical Communications, Simon Plass (ed.), ISBN 979-953-307-443-5

Haindl, B.; Rihacek, CHr.; Sajatovic, M.; Phillips, B.; Budinger, J.; Schnell, M.; Lamiano, D. & Wilson, W. (2009). Improvement of L-DACS1 Design by Combining B-AMC with P34 and WiMAX Technologies, Integrated Communications Navigation and Surveillance Conference (ICNS 2009), Arlington, VA, USA, May 2009

ICAO, ACP-WGC (2006). Report of the Tenth Meeting of ICAO ACP Working Group C, Montreal, 13-17 March 2006

ICAO, ACP-WGC (2011). FCS Phase II Results Paper 3 - Detailed Technology Investigations, Working Group C – 11th meeting, Brussels, Belgium, 18 – 20 September 2006

IICAO, ACP-WGW (2008). Report of the Working Group of the Whole, Second Meeting, Montreal, 21 to 25 April 2008

Matolak D.W., Sen I., Xiong W. (2008). The 5GHz Airport Surface Area Channel Part I, Measurement and Modeling Results for Large Airports, *IEEE Trans. Vehicular Tech.*, vol. 57, no. 4, pp. 2014–2026, 2008

Rice, M.; Davis, A.; Bettweiser, C. (2004). Wideband Channel Model for Aeronautical Telemetry; *IEEE Trans. On Aerospace and Electronic Systems*, vol. 40, no.1, January 2004

SESAR JU (2011). Updated LDACS1 System Specification. Information available at www.sesarju.eu

Zhidkov, S.V. (2006). Performance Analysis and Optimization of OFDM Receiver with Blanking Nonlinearity in Impulsive Noise Environment, *IEEE Transactions on Vehicular Technology,* Vol. 55, No. 1, (January 2006), pp. 234–242

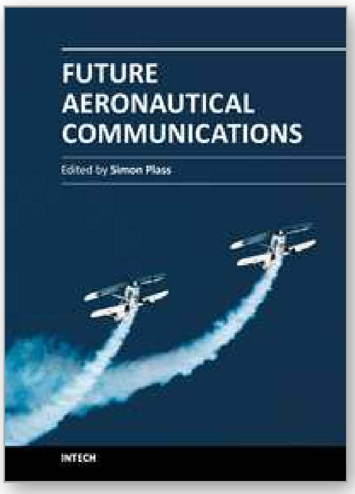

Future Aeronautical Communications

Edited by Dr. Simon Plass

ISBN 978-953-307-625-6

Hard cover, 378 pages

Publisher InTech

Published online 26, September, 2011

Published in print edition September, 2011

There are well-founded concerns that current air transportation systems will not be able to cope with their expected growth. Current processes, procedures and technologies in aeronautical communications do not provide the flexibility needed to meet the growing demands. Aeronautical communications is seen as a major bottleneck stressing capacity limits in air transportation. Ongoing research projects are developing the fundamental methods, concepts and technologies for future aeronautical communications that are required to enable higher capacities in air transportation. The aim of this book is to edit the ensemble of newest contributions and research results in the field of future aeronautical communications. The book gives the readers the opportunity to deepen and broaden their knowledge of this field. Todayâ€™s and tomorrowâ€™s problems / methods in the field of aeronautical communications are treated: current trends are identified; IPv6 aeronautical network aspect are covered; challenges for the satellite component are illustrated; AeroMACS and LDACS as future data links are investigated and visions for aeronautical communications are formulated.